Title

Expression and characterization of an epoxide hydrolase from Anopheles gambiae with high activity on epoxy fatty acids

Authors

Xu, Jiawen
Morisseau, Christophe
Hammock, Bruce D

Publication Date

2014-11-01

DOI

10.1016/j.ibmb.2014.08.004

Peer reviewed

Published in final edited form as:
Insect Biochem Mol Biol. 2014 November ; 54: 42–52. doi:10.1016/j.ibmb.2014.08.004.

Expression and characterization of an epoxide hydrolase from *Anopheles gambiae* with high activity on epoxy fatty acids

Jiawen Xu, **Christophe Morisseau**, and **Bruce D. Hammock***
Department of Entomology and Nematology, UC Davis Comprehensive Cancer Center University of California, Davis CA 95616, USA

Abstract

In insects, epoxide hydrolases (EHs) play critical roles in the metabolism of xenobiotic epoxides from the food resources and in the regulation of endogenous chemical mediators, such as juvenile hormones. Using the baculovirus expression system, we expressed and characterized an epoxide hydrolase from *Anopheles gambiae* (AgEH) that is distinct in evolutionary history from insect juvenile hormone epoxide hydrolases (JHEHs). We partially purified the enzyme by ion exchange chromatography and isoelectric focusing. The experimentally determined molecular weight and pI were estimated to be 35kD and 6.3 respectively, different than the theoretical ones. The AgEH had the greatest activity on long chain epoxy fatty acids such as 14,15-epoxyeicosatrienoic acids (14,15-EET) and 9,10-epoxy-12Z-octadecenoic acids (9,10-EpOME or leukotoxin) among the substrates evaluated. Juvenile hormone III, a terpenoid insect growth regulator, was the next best substrate tested. The AgEH showed kinetics comparable to the mammalian soluble epoxide hydrolases, and the activity could be inhibited by AUDA [12-(3-adamantan-1-yl-ureido) dodecanoic acid], a urea-based inhibitor designed to inhibit the mammalian soluble epoxide hydrolases. The rabbit serum generated against the soluble epoxide hydrolase of *Mus musculus* can both cross-react with natural and denatured forms of the AgEH, suggesting immunologically they are similar. The study suggests there are mammalian sEH homologs in insects, and epoxy fatty acids may be important chemical mediators in insects.

Please return comments and proofs to: Professor Bruce D. Hammock Department of Entomology University of California 1 Shields Avenue Davis, California 95616 Tel: 530-752-7519 Fax: 530-752-1537 bdhammock@ucdavis.edu. *Corresponding author. Tel.: +1 530 752 7519; fax: +1 530 752 1537. bdhammock@ucdavis.edu.

* Abbreviations: EH, epoxide hydrolase; JH, juvenile hormone; sEH, soluble epoxide hydrolase; mEH, microsomal epoxide hydrolase; JHEH, juvenile hormone epoxide hydrolase; AgEH, EH from *Anopheles gambiae*; HsEH, sEH from *Homo sapiens*; MsEH, sEH from *Mus musculus*; RsEH, sEH from *Rattus norvegicus*; SpEH1, sEH1 from *Strongylocentrotus purpuratus*; SpEH2, sEH2 from *Strongylocentrotus purpuratus*; AtEH, sEH from *Arabidopsis thaliana*; GsEH, sEH from *Glycine max*; StEH, sEH from *Solanum tuberosum*; CeEH1, sEH1 from *Caenorhabditis elegans*; CeEH2, sEH2 from *Caenorhabditis elegans*; HmEH, mEH from *Homo sapiens*; RmEH, mEH from *Rattus norvegicus*; DmEH, mEH from *Drosophila melanogaster*; MsJHEH, JHEH from *Manduca sexta*; BmJHEH-r1, JHEH-r1 from *Bombyx mori*, *c*-SO, *cis*-stilbene oxide; *t*-SO, *trans*-stilbene oxide; *t*-DPPO, *trans*-diphenylpropene oxide; EET, epoxyeicosatrienoic acids; EpOME, epoxy octadecenoic acids; AUDA, 12-(3-adamantan-1-yl-ureido) dodecanoic acid; *t*-TUCB, *trans*-4-{4-[3-(4-trifluoromethoxy-phenyl)-ureido]-cyclohexyloxy}-benzoic acid; TPPU, 1-trifluoromethoxyphenyl-3-(1-propionylpiperidin-4-yl) urea.

1. Introduction

Anopheles gambiae mosquitoes are the most important vectors of malaria, which is one of the most severe insect-borne diseases. Approximately 3.3 billion people worldwide are at risk from malaria, and it caused an estimated 627,000 deaths in 2012 (WHO, 2012). In order to understand the blood feeding behavior and the unique interactions between mosquitoes and their hosts, recent studies have found a variety of blood-derived factors that are ingested by female mosquitoes, and are still biologically active in the midgut. These blood components include some cytokines (TGF-β1), growth factors (insulin and insulin-like growth factors), pathogen derived molecules (glycosylphosphatidylinositols and hemozoin of *Plasmodium falciparum*) and others (Akman-Anderson et al., 2007; Beier et al., 1994; Lim et al., 2005; Surachetpong et al., 2009). These blood-derived molecules can trigger the conserved signaling pathways in mosquitoes to affect mosquito physiology, like aging, reproduction, immune responses and disease transmission patterns (Pakpour et al., 2013), which can critically affect the capacity of mosquitoes as disease vectors. To fully comprehend the interactions between mosquitoes and their hosts, additional blood factors need to be identified and their functions studied.

Epoxy fatty acids and their corresponding diols are autocrine and paracrine signaling molecules. Epoxyeicosatrienoic acids (EETs) are epoxygenated metabolites of C-20 arachidonic acid, and EETs belong to a group of potent chemical mediators termed eicosanoids. Together with prostaglandins and leukotrienes, these eicosanoids have been extensively studied in the mammalian systems in the context of human health and drug development (Morisseau and Hammock, 2013; Tapiero et al., 2002). In insects it is known that eicosanoids are also involved in insect physiology such as ion transport, reproduction and immunity (Stanley, 2006; Stanley and Kim, 2014; Stanley and Miller, 2006)

Epoxy fatty acids are endogenous substrates in mosquitoes. Like mammals, mosquitoes may synthesize epoxides of unsaturated fatty acids by a variety of cytochrome p450 enzymes. In addition, epoxy fatty acids are regular components of mammalian blood (Imig, 2012; Jiang et al., 2012; Jiang et al., 2005), and may be xenobiotic substrates for the female mosquitoes during blood feeding.

In mammals, EETs are short-lived lipid signaling molecules, and are mainly hydrolyzed by the soluble epoxide hydrolase (sEH), which was discovered while studying the mammalian metabolism of insect juvenile hormone and its analogs (Gill et al., 1974; Gill et al., 1972). The sEH turned out to be a therapeutic target for a variety of mammalian diseases (Imig, 2005; Imig and Hammock, 2009; Schmelzer et al., 2005; Zhang et al., 2007). In insects, epoxide hydrolases with activities on juvenile hormones (JHEHs) are the best characterized EHs (Anspaugh and Roe, 2005; Keiser et al., 2002; Khalil et al., 2006; Seino et al., 2010; Tsubota et al., 2010; Zhang et al., 2005). These EHs are believed to be involved in the metabolic degradation of juvenile hormones *in vivo* (Li et al., 2004; Prestwich et al., 1996), which are key developmental and reproductive hormones (Goodman and Cusson, 2011). So far, the insect mEHs and JHEHs characterized are homologous to mammalian microsomal epoxide hydrolases (Newman et al., 2005; Prestwich et al., 1996). The homologs of mammalian soluble epoxide hydrolases in insects have not been studied to our knowledge,

although the sEH homologs had been reported in the *C. elegans* (Harris et al., 2008). The AgEH characterized here shows evolutionary, biochemical, and immunological similarities to mammalian sEHs, suggesting there are sEH homologs in insects, and epoxy fatty acids may be important chemical mediators for insects. The biochemical characterization from this study provides knowledge and tools to pave the road for investigating whether epoxy fatty acids (such as EETs, known for biomedical studies from mammals) play a profound role in mosquito biology.

2. Materials and methods

2.1. Phylogeny analysis

Protein sequences of previously reported epoxide hydrolases and putative mosquito EH sequences were obtained from the database in the National Center for Biotechnology. Sequences were aligned and compared by ClustalW Omega. The phylogeny tree was generated using MEGA Version 5.2.1 (Tamura et al., 2011) with the Neighbor-Joining method (Saitou and Nei, 1987). 26 EH sequences were employed to infer the bootstrap consensus tree from 1000 replicates (Felsenstein, 1985). The percentage of replicate trees in which the associated taxa clustered together in the bootstrap test (1000 replicates) is shown next to the branches. The evolutionary distances were computed using the Poisson correction method.

2.2. Generation of recombinant virus

Many epoxide hydrolases have been successfully expressed in the baculovirus system by insect cells. We also chose to express the AgEH with this eukaryotic expression system. The sf-9 cell lines are of insect origin, and we did not detect significant background epoxide hydrolase activities with the substrates used under the assay conditions. The open reading frame sequence (AGAP 011972) was purchased from GenScript (Piscataway, NJ). Primers were designed to add Bgl II and EcoR I endonuclease-cutting sites at the N-terminal and C-terminal end, respectively. There were no tags added. The insert was cloned into the transfer vector pAcUW 21 (Weyer et al., 1990) by T4 DNA ligase (New England Biolabs, MA). Recombinant baculoviruses were generated by co-transfection of insect Sf9 cells with *Bsu 36 I*-digested BacPak 6 viral DNA (Clontech, CA) and the transfer vector pAcUW 21. Recombinant viruses were amplified and isolated by three consecutive plaque assays to ensure consistency. The titer of final recombinant viruses was determined by plaque assays, which was 5.4×10^8 pfu/ml.

2.3. Baculovirus expression and differential centrifugation

Control recombinant CpJHE baculoviruses and recombinant AgEH baculoviruses were used to infect insect Sf-9 cells, which were grown to a density of 1×10^6 cells/ml in Ex-cell 420 serum free medium (Sigma-Aldrich, MO) with 1% Pen/Step antibiotics (Sigma-Aldrich, MO) in a 50 ml shaker. The two recombinant viruses were generated in the same way, except that the inserted genes were different. Cells infected by CpJHE will express an esterase (Kamita et al., 2011) instead of an epoxide hydrolase. Virus (10 M.O.I) was added, and cells were harvested two days post infection.

All of the following operations were carried out at 4°C or lower. Infected cells were pelleted at 100×g for 10 minutes and resuspended in pH 8, 50 mM Tris buffer with 1 mM EDTA and 1 mM PMSF. A Polytron homogenizer (6000 rpm for 60 s) was used to break the cells. The crude homogenates were centrifuged at 800×g for 10 minutes to remove cell debris, and the supernatant was centrifuged at 17,000×g for 20 minutes to spin down mitochondria and peroxisome fractions. Then the supernatant was subjected to 100,000×g for 60 minutes. The resulting supernatant was collected as the cytosolic fraction, and the pellet resuspended in Tris buffer containing 0.02% CHAPS as the microsomal fraction. For each step, the pellets were washed once by Tris buffer before any further processing. Protein concentrations were determined by the BCA protein assay (Pierce, IL) throughout this study with BSA as the standard.

2.4. Optimal pHs for enzyme activity and stability

In order to investigate the effects of pH on enzyme activity and stability, cells were disrupted in different buffers. Sodium acetate (pH 5 and 6), Bis-Tris (pH 6 and 7), phosphoric buffer (pH 7 and 8), Tris (pH 8 and 9), borate (pH 9 and 10), CAPS (pH 10 and 11) were chosen to cover the pH range between 5 to 11. All buffers were 50 mM in concentration and sodium chloride was added accordingly to make constant ionic strength at 100mM for each buffer. Enzyme activity was detected with *t*-DPPO as the substrate.

2.5. Effect of ionic strength and inhibitors on enzyme activity

Sodium chloride solutions (0 mM to 3000 mM) were prepared and added into 50 mM Tris buffers, pH 8 to adjust the ionic strength between 50 mM −2000 mM. The effects of ionic strength (50 mM −2000 mM) on enzyme activity were detected with *t*-DPPO, juvenile hormone III and 14,15-EET as the substrate (Morisseau, 2007).

Six small molecule inhibitors of different structural classes were used to study the inhibition patterns of the recombinant AgEH. The synthesis, chemical and physical properties of these compounds are described somewhere else (Morisseau et al., 1999; Morisseau et al., 2002; Severson et al., 2002). Inhibitors were prepared in DMSO. 1 μl of inhibitors at the appropriate concentration was added into 100 μl enzyme solutions before addition of substrates (*t*-DPPO, JH III or 14,15-EET). 1 μl of DMSO was added into enzyme solutions as a control, although inhibition by DMSO was not observed at 1% (v/v) concentration. Enzymes from the microsomal fractions were used, and the incubation time was 5 min.

2.6. Solubilization of AgEH activity from the membrane

Enzymes were obtained by disrupting insect Sf-9 cells two days after infection by baculoviruses at a M.O.I of 10. Microsomes were prepared as described in Section 2.3. Multiple conditions were evaluated to release the enzyme from the membrane, including high salt buffer (sodium chloride, 0 M-3 M), urea (1 M), sonication (3×30 seconds) and detergents (Triton-X100, CHAPS at varied concentrations). The microsomes were treated and incubated for one hour at 4 °C. The solution was centrifuged again at 100,000×g for 1 hour. The enzyme activity in the supernatant and pellet was measured with *t*-DPPO as the substrate.

2.7. Enzyme assays and determination of kinetics

c-SO, *t*-SO, *t*-DPPO and JH III were tritium-labeled epoxide hydrolase substrates. The enzyme activity was determined by partition assays as previously described (Borhan et al., 1995; Gill et al., 1983a; Mumby and Hammock, 1979). Briefly 1 μl of 5 mM *c*-SO, *t*-SO, *t*-DPPO, 14,15-EET, 9,10-EpOME or 0.5 mM JH III substrates in DMSO were added into 100 μl of the appropriately diluted enzyme solutions with 0.1 mg/ml BSA. For 9,10-EpOME and 14,15-EET, the enzyme incubation was similar to tritium-labeled compounds, but the products were analyzed by LC-MS/MS (Morisseau, 2007).

The enzyme kinetics was studied using *t*-DPPO, JH III and 14,15-EET as substrates. A wide range of substrate concentrations was first employed to determine the approximate range of the K_m. Then five more specific substrate concentrations covering the range $K_m/5$ to $5\times K_m$ were used. Enzymes were diluted accordingly, and incubated for 5min, 10 min and 30 min at 30°C in a water bath. Each assay was run in triplicate, and all the data within the linear range were included in subsequent calculations (Morisseau, 2007). The kinetics was determined by three independent experiments. As a result, for each substrate concentration, at least 9 datum points were available for the software SigmaPlot (Systat Software, CA) to fit the Michaelis-Menton equation.

2.8. Partial purification of AgEH by ion exchange chromatography and isoelectric focusing

Solubilized AgEH fractions following treatment with 0.3% CHAPS were used as the starting materials, and was assigned as 100% activity. Prepacked Q-Sepharose columns (GE healthcare, CA) were washed by 10 column volumes of starting buffer, which contains 20 mM, pH 8 Tris-HCl, 0.3% CHAPS and 10% glycerol. Solubilized AgEH fractions were loaded with a syringe, and the flow through was collected. The column was then washed by 5 column volumes of starting buffer, and then NaCl gradients (0.2 M-1 M). The flow rate was controlled at 1 ml/min.

The NaCl eluate with the highest enzyme specific activity was desalted by ultrafiltration (Amicon Ultra, 10K NMWL), and reconstituted with pure water to the final volume of 60 ml, which contained 2% (w/v) pH 3-10 ampholytes (Bio-Rad, CA), 0.3% CHAPS and 10% glycerol. In a cold room with temperature set at 4°C, samples were loaded on the Rotofor cell (Bio-Rad, CA), and focusing was run at 10W constant power with a cooling circulator set at 4°C for 4 hours. The initial conditions were 500 V and 20 mA. At equilibrium the values were 2000 V and 5 mA. 20 Rotofor fractions were collected by vaccum aspiration. The pH of each fraction was measured at 4°C using a Corning 430 pH meter. The pH was adjusted to 8 by adding 100 μl of fraction solutions to 900 μl of 50 mM, pH 8 Tris buffer. The specific activity of each fraction was then measured with *t*-DPPO as the substrate.

2.10. SDS-PAGE and western blot analysis of purification fractions

Solubilized enzymes (S), 0.2M NaCl Q-Sepharose eluate and a selection of Rotofor fractions (#3-#13) were loaded on a 4-20% Tris-glycine gel (Life Technologies, CA), and stained by Sypro® Ruby Red stain (Life Technologies, CA). The proteins were also transferred to a nitrocellulose membrane by the Pierce G2 Fast Blotter (Thermo Scientific, IL). The membrane was blocked by 1% milk in Tris-buffered saline with 0.1% tween 20

(TBST) at room temperature for one hour, and blotted against a 1/10000 diluted polyclonal mouse sEH antibody (Imig et al., 2002) in TBST at 4°C overnight. The antibody was screened and found to have cross-reactivity with the AgEH (Fig. S4). The membrane was then washed in TBST and incubated with the 1/10000 diluted goat anti-rabbit secondary antibody conjugated to horseradish peroxidase (Abcam, UK). Detection was achieved by incubating the membrane with SuperSignal® West PicoChemiluminescent Substrate (Thermo Scientific, IL) and exposing blot to an X-ray film for one minute.

2.11. Immunoprecipitation of the AgEH activity

20 μL of Pierce Protein A/G Plus Agarose slurry (10 μL of settled resin) was added into a microcentrifuge tube, and washed by 1X coupling buffer (Pierce, IL). Absorption at 280 nm was used to estimate the protein concentration of the rabbit anti-mouse sEH serum (Imig et al., 2002). The serum varying from 30 μg to 1200 μg total IgG was added into the tube. The agarose-antibody mixture was incubated on a rotator at room temperature for 60 minutes. The tube was subject to centrifugation at 1,000×g for 2 minutes at 4 °C, and the supernatant was discarded. The resin was then washed twice by 1X coupling buffer. The solubilized AgEH solution was pre-cleared by incubating 500 μL of the solubilized AgEH with the control agarose resin (Pierce, IL) at 4 °C for 60 minutes with gentle end-over-end mixing. The pre-cleared solution was then added to the agarose resin coupled with mouse sEH serum. The mixture was incubated overnight at 4 °C. After the incubation, the tube was centrifuged, and the supernatant was collect for measuring the AgEH activity with *t*-DPPO as the substrate.

3. Results

3.1. Phylogeny analysis of the epoxide hydrolase from *Anopheles gambiae* (AgEH)

Most epoxide hydrolases studied belong to the α/β hydrolase family, which share similar three-dimensional structures and enzymatic mechanism (Morisseau and Hammock, 2005; Newman et al., 2005). Based on such structural and enzymatic similarities, *in silico* studies of the genome *of Anopheles gambiae* revealed one putative insect epoxide hydrolase (AGAP 011972) that was distinct from insect mEHs and JHEHs in homology. The resulting sequence (AGAP 011972, showed in Fig. S1) contained conserved catalytic triad (D-159, H-319, D-291), oxyanion hole motif (HGXP, residues 90-93) and two tyrosines (Y-206, Y-261), which are all signature elements for epoxide hydrolases to function.

In the phylogenic analysis (Fig. 1), the AgEH was clustered with putative EH sequences from the other two medically important mosquitoes, *Aedes aegypti* (2 sequences, prefixed with ‘AAEL’) and *Culex quinquefasciatus* (5 sequences, prefixed with ‘CPIJ’). Except for the orthologs in mosquitoes, the AgEH was most close to soluble epoxide hydrolases from *Caenorhabditis elegans* (CeEH 1 and 2), EH 3 and EH 4 from *Homo sapiens*. It was also homologous to soluble epoxide hydrolase from plants (AtEH, from cress *Arabidopsis thaliana*; StEH, from potato *Solanum tuberosum* and GsEH, from soybean *Glycine max)* to a lesser extent. These epoxide hydrolases contained the conserved C-terminal epoxide hydrolase domain of sEHs from mammals (Arahira et al., 2000; Morisseau et al., 2000), but lacked the N-terminal phosphatase domain. Among all the sequences analyzed, the AgEH

was remotely related to the reported microsomal EH homologs, including mammalian microsomal EHs (RmEH, from rat *Rattus norvegicus*; HmEH, from human *Homo sapiens*), mainly known for their role in detoxification (Morisseau and Hammock, 2008), a microsomal EH (DmEH, from fruit fly *Drosophila melanogaster*) that cannot hydrolyze juvenile hormones (Taniai et al., 2003), and also insect JHEHs (MsJHEH, from the tobacco horn worm *Manduca sexta*; BmJHEH-r1, from silkworm *Bombyx mori*) that have a high hydrolytic activity on juvenile hormones (Seino et al., 2010; Touhara et al., 1994). There are also three putative JHEH sequences in the tree (prefixed with AGAP), and they all clustered with previously reported insect mEHs and JHEHs.

3.2. Substrate selectivity of AgEH

We moved on to test the hypothesis that the sequence AGAP 011972 did code for a catalytically active epoxide hydrolase. The enzyme was expressed in insect Sf-9 cells infected by 10 M.O.I recombinant AgEH viruses or recombinant CpJHE viruses as a control. The reported data were corrected for non-enzymatic hydration in the assays (Fig. S2). Epoxide hydrolase activity detected in cell lysate from the CpJHE virus infection was about 700-1000 times lower than the cell lysate from the AgEH virus infection (Fig. S2).

The structures of epoxide substrates are shown (Fig. 2). There was no activity greater than the non-enzymatic hydrolysis of *c*-SO and *t*-SO in cells infected by the recombinant AgEH viruses (Table 1). Although a typical substrate for many mammalian and insect microsomal EHs (Gill et al., 1983b; Kamita et al., 2013; Morisseau and Hammock, 2005; Taniai et al., 2003), *c*-SO was not a substrate for the AgEH. However, the AgEH was catalytically active on JH III (98 nmol diol formed×min^{-1}×mg^{1} protein), *t*-DPPO (564 nmol diol formed×min^{-1}×mg^{-1} protein), 14,15-EET (550 nmol diol formed×min^{-1}×mg^{-1} protein) and 9,10-EpOME (360 nmol diol formed×min^{-1}×mg^{-1} protein). *t*-DPPO is a commonly used surrogate substrate for mammalian soluble epoxide hydrolase, and is not an endogenous substrate in insects either. JH III is a proven important insect chemical mediator that insect EHs can hydrolyze. 14,15-EET and 9,10-EpOME are proposed to be endogenous substrates for the mammalian sEHs. Potentially they may be the endogenous and xenobiotic substrates (during blood feeding) for mosquitoes as well.

3.3. The subcellular locations of AgEH

Next we determined the subcellular location of the AgEH expressed in Sf-9 cells by detecting enzyme activity on *t*-DPPO. Cells infected by 10 M.O.I viruses were harvested at 48 hours after infection, and differential centrifugation was proceeded as previously described. In insect Sf-9 cells, the AgEH appeared to be a membrane-associated protein (Table 2), because when the activity of the crude cell lysate was assigned a value of 100%, 27% and 48% activity was recovered from the mitochondrial (peroxisomal) and the microsomal fraction respectively. Only 3% activity was detected in the 100,000×g cytosolic fraction. The enzyme was three times more concentrated in the microsomes than in the crude cell lysate.

3.4. Effects of pH on enzyme activity and stability

The enzyme activity is buffer and pH dependent (Fig. 3). At pH 5, there was no activity detected. The highest specific activity was achieved from enzymes in Bis-Tris buffer, pH 7, followed by Tris buffer at pH 9 and 8. However, the enzyme was more stable in Tris buffer than it was in Bis-Tris during the first three weeks (Fig. 4). In Tris buffer pH 9, the activity was not lost in the first week. At week 3, there was still 70% activity remained. The enzymes in different buffer and pH conditions were all stored in a bucket of crushed ice in a 4 °C freezer. Storing enzyme at −80°C and thawing (in pH 8, Tris buffer) caused more than 50% total activity loss the first day (data not shown).

3.5. The inhibition patterns

Among the 6 inhibitors chosen for evaluation (Fig. 5), AUDA, *t*-TUCB and TPPU (#1 to #3) are urea-based mammalian sEH inhibitors (Morisseau et al., 1999). Elaidamide (#4) is a potent microsomal EH inhibitor (Morisseau et al., 2008). #5 and #6 are two potent inhibitors for the JHEH from *Manduca sexta* (Severson et al., 2002). AUDA was the most potent inhibitor for all the three substrates tested (Table 3). AUDA inhibited 90.5%, 88.8% and 65.3% of the enzyme activity on *t*-DPPO, JH III and 14,15-EET respectively at a concentration of 50 nM. The IC_{50} of AUDA on 14,15-EET was estimated to be 60 nM (Fig. 6). TPPU (#3) and elaidamide (#4) had no significant inhibition even at 500 nM concentrations. JHEH inhibitors (#5 and #6) also showed inhibition for the three substrates, probably due to their structural similarity to juvenile hormones, which are substrates to the AgEH.

3.6. Enzyme kinetics

Then we evaluated the kinetics of the AgEH on the four substrates. We also compared the kinetics of other EHs on these substrates (Table 4). Cited kinetic values of JHEH from *Manduca sexta* are from Severson and Touhara (Severson et al., 2002; Touhara et al., 1994), while the kinetic data of the soluble epoxide hydrolase from *H.sapiens* are from Morisseau (Morisseau et al., 2000; Morisseau et al., 2010)

Based on the V_{max}/K_m ratio, the best substrate among the four tested is 14,15-EET, and the least preferred is *t*-DPPO. The ratio on 14,15-EET was 0.46 $L\times min^{-1}\times mg^{-1}$ protein, which was 2.2 fold, 3.5 fold and 11 fold higher than those of 9,10-EpOME, JH III and *t*-DPPO respectively.

The kinetics of AgEH on 14,15-EET and 9,10-EpOME is comparable to the soluble epoxide hydrolase from *H.sapiens*, to which epoxy fatty acids are considered the endogenous substrates (Yu et al., 2000; Zeldin et al., 1993). The V_{max}/K_m of AgEH on 14, 15-EET and 9,10-EpOME were slightly higher (2.3 and 1.6 times respectively) than that of sEH from *H.sapiens*, even considering that a crude microsomal fraction was used to determine the kinetics. The AgEH and the sEH from *H.sapiens* can both hydrolyze juvenile hormone III, at a lower V_{max}/K_m ratio than on epoxy fatty acids. The JHEH from *Manduca sexta* hydrolyzed JH III with a low K_m (0.28μM) and a low V_{max} (0.095 $\mu mol\times min^{-1}\times mg^{-1}$proteins) while AgEH hydrolyzed JH III with a high K_m (9.8 μM) and a high V (1.3 $\mu mol\times min^{-1}$ max $\times mg^{-1}$proteins). For *t*-DPPO, the V_{max}/K_m of AgEH was 8

times lower than that of human sEH, but 46 times higher than that of MsJHEH. 3.6. Solubilization of AgEH activity from the membrane.

In order to solubilize the AgEH from the membrane, high salt buffers, urea, sonication were first evaluated to release the enzyme from the membrane. High salt buffer (sodium chloride at 0-3 M), urea (1 M) and sonication (3×30 seconds) did not release a significant amount of enzyme activity from the membrane (Table 5), which suggested that the enzyme was not loosely bound with the membrane.

Then we tried to solubilize the enzyme with two detergents (Triton X-100 and CHAPS), and the result is shown (Table 6). The addition of 0.3% CHAPS was detrimental to the activity (49% recovery from resuspended microsomes), but could solubilize 75% of recovered enzyme activity to the supernatant, while in lower concentrations (0.01%- 0.1%), the majority of activity was still in the pellets. Triton X-100 was not as efficient as CHAPS in solubilizing AgEH activity in terms of recovery and solubilized activity (33% maximum).

3.7. Partial purification of the AgEH and analysis of purification fractions by SDS-PAGE and western blot

The starting material was 40 ml solubilized enzyme fractions with a total activity of 52 U (1 U=1 μmol/min) and a specific activity of 0.18 U/mg protein (Table 7). The 0.2M NaCl Q-Sepharose eluate contained 67% of total activity but only achieved 1.7 fold of purification, and lower specific activities were also detected in other fractions (Fig. S3). Ionic strength from 0.05 M to 2 M did not have a significant effect on enzyme activity when *t*-DPPO was used as the substrate (Table. S1). The #7 Rotofor fraction had a total activity of 5 U and a specific activity of 3.13U/mg proteins. Thus, the purification factor was 17 fold with 10% recovery (Table 7).

The cDNA of the AgEH (AGAP 011972) is 1492bp long with a deduced 340 amino acid sequence (Fig. S1). The predicted molecular mass and pI are 40.9 kD and 9.2 respectively (Artimo et al., 2012). The Rotofor determined pI of the AgEH was 6.3. High specific activities were detected in fraction #4, 5, 6, 7, 8, and the highest activity was found in fraction #7, which had a pH of 6.3 (Fig. 7). When proteins were loaded on a 4-20% gradient Tris-glycine SDS-PAGE gel (Life Technologies, CA), and the PageRuler Unstained Protein ladder (Thermo Scientific, MA) was used as the marker, a band approximate 35kD (Fig. 8a) was found to correlate well with the enzyme activity detected in different fractions. The band was also recognized by a rabbit serum against mouse soluble epoxide hydrolase (Fig. 8b). The rabbit serum also recognized a band approximates 35kD in the crude lysate of insect cells (Fig. S4) infected by the recombinant AgEH baculoviruses, but not lysate of the CpJHE infected cells (Fig. S4), which expresses a recombinant juvenile hormone esterase from *Culex quinquefasciatus*. The CpJHE viruses were generated in the same way as the AgEH, except for that the inserted gene was different (Kamita et al., 2011). The band was also cut for protein sequencing (UC Davis Proteomics Core), which was digested by trypsin. The data were analyzed by Scaffold version 4.3.2 (Proteome Software Inc., OR) based on peptide and protein identifications. The protein sequence of the AgEH was identified with 100% probability to a false discover rate less than 0.1% and 1.0% for peptide and protein identifications (Nesvizhskii et al., 2003) respectively.

3.8. Immunoprecipitation of the AgEH activity

The result of immunoprecipitation study is shown (Fig. 9). When a constant amount of the solubilized AgEH was incubated with a varying amount of rabbit anti-mouse sEH serum, the AgEH activity was precipitated in a dose-dependent manner, indicating the natural form of the AgEH also cross-reacted with the rabbit serum. Elution of the AgEH by low pH and high salt buffer had not been successful, and elution by SDS loading buffer resulted in a large contamination of antibodies and other proteins. Therefore, we have not obtained a homogenous and catalytically active AgEH.

Discussion

The AgEH has a different evolutionary history from insect mEHs and JHEHs. They share the same subcellular location, but have complementary and overlapping substrate selectivities. As a result, EH activities detected from a specific subcellular location cannot be simply assigned to one enzyme.

The AgEH orthologs are also found in the genome of *Aedes aegypti* and *Culex quinquefasciatus*, two medically important mosquitoes as well as *Anopheles gambiae*. Interestingly, we were not able to find orthologs and activities on EETs in *Drosophila melanogaster*. The orthologs all share an evolution different than the previously characterized insect JHEHs and mEHs. The catalytic triad (Asp-Asp-His) present in the orthologs is more commonly seen in sEHs. It is tempting to characterize the orthologs in *Aedes aegypti* and *Culex quinquefasciatus*, and determine whether the orthologs are EHs, whether they can hydrolyze epoxy fatty acids or juvenile hormones, and whether the inhibitor and antibody described in this study can be useful tools.

The substrate selectivity (structures showed in Fig. 2) suggests the AgEH hydrolyze 1,2-disubstituted epoxides (*t*-DPPO, 14,15-EET, 9,10-EpOME) better than tri-substituted epoxides (JH III), and the AgEH does not hydrolyze epoxides that are sterically hindered on both sides by bulky groups (*c*-SO and *t*-SO). The kinetics and inhibition patterns both show that epoxy fatty acids are preferred substrates among those that tested, and sEH inhibitor AUDA is the most potent inhibitors among the inhibitors evaluated. However, we can not exclude the possibility that the AgEH may involve in the metabolism of juvenile hormone in certain conditions. While juvenile hormone esterases are secreted to the hemolymph (Kamita and Hammock, 2010), membrane-associated epoxide hydrolases may have a significant kinetic advantage regulating juvenile hormone titer within cells. Comparing the AgEH to the well-studied JHEH from *Manduca sexta*, there are enormous differences in the K_m and V_{max}, while their catalytic efficiencies are within the same range (Table 4). When the titer of juvenile hormones increases, the capacity of the JHEH to regulate juvenile hormone metabolism may be strongly limited as the titer surpasses the low K_m of the JHEH. Meanwhile, the contribution of the AgEH to juvenile hormone metabolism may be significant because it has a high V_{max}, and a high K_m that lies at a point that juvenile hormone titer is probably not able to reach. As a result, the AgEH may play a role in regulating juvenile hormone titer under conditions that a high juvenile hormone titer is present locally and need to be dramatically down-regulated.

In our case, the experimentally determined molecular weight (around 35kD) and pI (6.3) were different from the theoretical ones (41kD, 9.2). It is not uncommon that amino acid sequences are used to predict the molecular weight and pI in biochemical studies, but amino acid sequences cannot be used to predict the three-dimensional structure and the post-translational modifications (cleavage of signal peptide, glycosylation, attachment of lipid), which can lead to miscalculation of physical properties, such as molecular weight and pI. As a membrane-associated enzyme, the AgEH is expected to contain a signal peptide that is cleaved during protein folding and processing, which may be the reason a smaller molecular weight was detected than the predicted molecular weight.

The rabbit serum for the mouse sEH can both detect the denatured and natural form of the AgEH, indicating immunologically the AgEH is similar to the mouse sEH. Although the overall homology between the AgEH and mammalian sEHs is relatively low (20-30%) (Table S2), the AgEH may also share similar three-dimensional structure with the mammalian enzymes. Proteins with low sequence homology but similar structures have been reported before (Dickerson and Geis, 1983; Olsen et al., 1975). Epoxide hydrolases belong to the α/β hydrolase fold, the members of which shares no or low sequence homology, but have rather similar structures (Ollis et al., 1992). The similarities between the AgEH and mammalian sEHs in overall sequence homology, conserved catalytic triad, biochemistry and immunology clearly suggest that they have diverged from a common ancestor, and they have evolved to preserve similar epoxide hydrolase activities.

In mosquitoes, the epoxy fatty acids may also be endogenous lipid signaling molecules or xenobiotic blood factors. In mammals, epoxy fatty acids are lipid signaling molecules and players in immune responses. The EpOMEs (leukotoxin) and its corresponding diols have been reported to be a strong mediator of acute respiratory distress syndrome (ARDS) (Moghaddam et al., 1997), and EETs are anti-inflammatory molecules that exert its effect by reducing the activity of NF-κB (Inceoglu et al., 2011; Liu et al., 2005; Morin et al., 2010; Node et al., 1999). In mosquitoes, the Toll and Imd pathways are the major immune signaling pathways that are studied in the context of immunity and disease transmission. Both pathways are highly conserved and depend on the NF-κB transcription factor to play crucial roles in anti-pathogen defense (Silverman and Maniatis, 2001). Many immune genes were reported to be regulated by NF-κB, such as diptericin, cecropin, attacin, defensing as well as nitric oxide synthase (Dong et al., 2006; Hillyer and Estevez-Lao, 2010; Luna et al., 2006; Richman et al., 1997; Vizioli et al., 2000). As prostaglandins and metabolites from the LOX pathway have been reported to mediate insect immunity, the inhibitor and the antibody described in the study can be used to investigate whether epoxy fatty acids are players in insect immunity, how the immunity is regulated and how the disease transmission patterns will be impacted.

Supplementary Material

Refer to Web version on PubMed Central for supplementary material.

Acknowledgments

This work is supported in part by NIEHS Grant ES02710, NIEHS Superfund Grant P42 ES04699, the UC Davis Jastro-Shields Graduate Research Award and the China Scholarship Council. We gracefully thank Dr. Shizuo Kamita for reading the manuscript and providing tips on baculovirus expression system. We also thank Dr. Ahmet Inceoglu for detailed discussions and helpful suggestions.

References

Akman-Anderson L, Olivier M, Luckhart S. Induction of nitric oxide synthase and activation of signaling proteins in *Anopheles* mosquitoes by the malaria pigment, hemozoin. Infection and Immunity. 2007; 75:4012–4019. [PubMed: 17526741]

Anspaugh DD, Roe RM. Regulation of JH epoxide hydrolase versus JH esterase activity in the cabbage looper, *Trichoplusia ni*, by juvenile hormone and xenobiotics. Journal of Insect Physiology. 2005; 51:523–535. [PubMed: 15893999]

Arahira M, Nong VH, Udaka K, Fukazawa C. Purification, molecular cloning and ethylene-inducible expression of a soluble-type epoxide hydrolase from soybean (*Glycine max L. Merr*.). European Journal of Biochemistry. 2000; 267:2649–2657. [PubMed: 10785386]

Artimo P, Jonnalagedda M, Arnold K, Baratin D, Csardi G, de Castro E, Duvaud S, Flegel V, Fortier A, Gasteiger E, Grosdidier A, Hernandez C, Ioannidis V, Kuznetsov D, Liechti R, Moretti S, Mostaguir K, Redaschi N, Rossier G, Xenarios I, Stockinger H. ExPASy: SIB bioinformatics resource portal. Nucleic Acids Research. 2012; 40:W597–W603. [PubMed: 22661580]

Beier MS, Pumpuni CB, Beier JC, Davis JR. Effects of *para*-aminobenzoic acid, insulin, and gentamicin on *Plasmodium falciparum* development in *Anopheline* mosquitos (Diptera, Culicidae). Journal of Medical Entomology. 1994; 31:561–565. [PubMed: 7932602]

Borhan B, Mebrahtu T, Nazarian S, Kurth MJ, Hammock BD. Improved radiolabeled substrates for soluble epoxide hydrolase. Anal Biochem. 1995; 231:188–200. [PubMed: 8678300]

Dickerson RE, Geis I. Hemoglobin: Structure function evolution and pathology. The American Journal of Human Genetics. 1983; 35(4):781–782.

Dong Y, Aguilar R, Xi Z, Warr E, Mongin E, Dimopoulos G. 2006. Anopheles gambiae immune responses to human and rodent *Plasmodium* parasite species. PLoS Pathog. 2:e52. [PubMed: 16789837]

Felsenstein J. Confidence-limits on phylogenies - an approach using the bootstrap. Evolution. 1985; 39:783–791.

Gill SS, Hammock BD, Casida JE. Mammalian metabolism and environmental degradation of juvenoid 1-(4′-ethylphenoxy)-3,7-dimethyl-6,7-epoxy-*trans*-2-octene and related compounds. Journal of Agricultural and Food Chemistry. 1974; 22:386–395. [PubMed: 4840500]

Gill SS, Hammock BD, Yamamoto I, Casida JE. Preliminary chromatographic studies on the metabolites and photodecomposition products of the juvenoid 1-(4′ ethylphenoxy)-6, 7-epoxy-3, 7-dimethyl-2-octene. Insect Juvenile Hormones: Chemistry and Action. 1972:177–189.

Gill SS, Ota K, Hammock BD. Radiometric assays for mammalian epoxide hydrolases and glutathione s-transferase. Analytical Biochemistry. 1983a; 131:273–282. [PubMed: 6614459]

Gill SS, Ota K, Ruebner B, Hammock BD. Microsomal and cytosolic epoxide hydrolases in rhesus monkey liver, and in normal and neoplastic human liver. Life Sciences. 1983b; 32:2693–2700. [PubMed: 6855465]

Goodman W, Cusson M. L.I. G. The Juvenile Hormones. Insect Endocrinology. 2011:311–347.

Harris TR, Aronov PA, Jones PD, Tanaka H, Arand M, Hammock BD. Identification of two epoxide hydrolases in *Caenorhabditis elegans* that metabolize mammalian lipid signaling molecules. Archives of Biochemistry and Biophysics. 2008; 472:139–149. [PubMed: 18267101]

Hillyer JF, Estevez-Lao TY. Nitric oxide is an essential component of the hemocyte-mediated mosquito immune response against bacteria. Dev Comp Immunol. 2010; 34:141–149. [PubMed: 19733588]

Imig JD. Epoxide hydrolase and epoxygenase metabolites as therapeutic targets for renal diseases. American Journal of Physiology - Renal Physiology. 2005; 289:F496–F503. [PubMed: 16093425]

Imig JD. Epoxides and soluble epoxide hydrolase in cardiovascular physiology. Physiological Reviews. 2012; 92:101–130. [PubMed: 22298653]

Imig JD, Hammock BD. Soluble epoxide hydrolase as a therapeutic target for cardiovascular diseases. Nature Reviews Drug Discovery. 2009; 8:794–805.

Imig JD, Zhao X, Capdevila JH, Morisseau C, Hammock BD. Soluble epoxide hydrolase inhibition lowers arterial blood pressure in angiotensin II hypertension. Hypertension. 2002; 39:690–694. [PubMed: 11882632]

Inceoglu B, Wagner K, Schebb NH, Morisseau C, Jinks SL, Ulu A, Hegedus C, Rose T, Brosnan R, Hammock BD. Analgesia mediated by soluble epoxide hydrolase inhibitors is dependent on cAMP. Proceedings of the National Academy of Sciences of the United States of America. 2011; 108:5093–5097. [PubMed: 21383170]

Jiang H, Anderson GD, McGiff JC. The red blood cell participates in regulation of the circulation by producing and releasing epoxyeicosatrienoic acids. Prostaglandins & Other Lipid Mediators. 2012; 98:91–93. [PubMed: 22178722]

Jiang HL, Quilley J, Reddy LM, Falck JR, Wong PYK, McGiff JC. Red blood cells: reservoirs of *cis*- and *trans*-epoxyeicosatrienoic acids. Prostaglandins & Other Lipid Mediators. 2005; 75:65–78. [PubMed: 15789616]

Kamita SG, Hammock BD. Juvenile hormone esterase: biochemistry and structure. Journal of Pesticide Science. 2010; 35:265–274. [PubMed: 23543805]

Kamita SG, Samra AI, Liu JY, Cornel AJ, Hammock BD. Juvenile hormone (JH) esterase of the mosquito *Culex quinquefasciatus* is not a target of the JH analog insecticide methoprene. PloS one. 2011; 6(12):e28392. [PubMed: 22174797]

Kamita SG, Yamamoto K, Dadala MM, Pha K, Morisseau C, Escaich A, Hammock BD. Cloning and characterization of a microsomal epoxide hydrolase from *Heliothis virescens*. Insect Biochemistry and Molecular Biology. 2013; 43:219–228. [PubMed: 23276675]

Keiser KCL, Brandt KS, Silver GM, Wisnewski N. Cloning, partial purification and in vivo developmental profile of expression of the juvenile hormone epoxide hydrolase of *Ctenocephalides felis*. Archives of Insect Biochemistry and Physiology. 2002; 50:191–206. [PubMed: 12125060]

Khalil SMS, Anspaugh DD, Roe RM. Role of juvenile hormone esterase and epoxide hydrolase in reproduction of the cotton bollworm, *Helicoverpa zea*. Journal of Insect Physiology. 2006; 52:669–678. [PubMed: 16678198]

Li S, Jiang R, Cao M. Metabolism of juvenile hormone. Acta Entomologica Sinica. 2004; 47:389–393.

Lim JH, Gowda DC, Krishnegowda G, Luckhart S. Induction of nitric oxide synthase in *Anopheles stephensi* by *Plasmodium falciparum:* Mechanism of signaling and the role of parasite glycosylphosphatidylinositols. Infection and Immunity. 2005; 73:2778–2789. [PubMed: 15845481]

Liu Y, Zhang Y, Schmelzer K, Lee T-S, Fang X, Zhu Y, Spector AA, Gill S, Morisseau C, Hammock BD, Shyy JY-J. The antiinflammatory effect of laminar flow: The role of PPARγ, epoxyeicosatrienoic acids, and soluble epoxide hydrolase. Proceedings of the National Academy of Sciences of the United States of America. 2005; 102:16747–16752. [PubMed: 16267130]

Luna C, Hoa NT, Lin H, Zhang L, Nguyen HL, Kanzok SM, Zheng L. Expression of immune responsive genes in cell lines from two different Anopheline species. Insect Mol Biol. 2006; 15:721–729. [PubMed: 17201765]

Moghaddam MF, Grant DF, Cheek JM, Greene JF, Williamson KC, Hammock BD. Bioactivation of leukotoxins to their toxic diols by epoxide hydrolase. Nature Medicine. 1997; 3:562–566.

Morin C, Sirois M, Echave V, Albadine R, Rousseau E. 17,18-epoxyeicosatetraenoic acid targets PPAR-gamma and p38 mitogen-activated protein kinase to mediate its anti-inflammatory effects in the lung: role of soluble epoxide hydrolase. American journal of respiratory cell and molecular biology. 2010; 43:564–575. [PubMed: 20008283]

Morisseau C. Measurement of soluble epoxide hydrolase (sEH) activity. Current Protocols in Toxicology. 2007; 33:34.23:34.23.31–34.23.18.

Morisseau C, Beetham JK, Pinot F, Debernard S, Newman JW, Hammock BD. Cress and potato soluble epoxide hydrolases: Purification, biochemical characterization, and comparison to

mammalian enzymes. Archives of Biochemistry and Biophysics. 2000; 378:321–332. [PubMed: 10860549]

Morisseau C, Goodrow MH, Dowdy D, Zheng J, Greene JF, Sanborn JR, Hammock BD. Potent urea and carbamate inhibitors of soluble epoxide hydrolases. Proceedings of the National Academy of Sciences of the United States of America. 1999; 96:8849–8854. [PubMed: 10430859]

Morisseau C, Goodrow MH, Newman JW, Wheelock CE, Dowdy DL, Hammock BD. Structural refinement of inhibitors of urea-based soluble epoxide hydrolases. Biochemical Pharmacology. 2002; 63:1599–1608. [PubMed: 12007563]

Morisseau C, Hammock BD. Epoxide hydrolases: mechanisms, inhibitor designs, and biological roles. Annual review of pharmacology and toxicology. 2005; 45:311–333.

Morisseau C, Hammock BD. Gerry Brooks and epoxide hydrolases: four decades to a pharmaceutical. Pest Management Science. 2008; 64:594–609. [PubMed: 18383502]

Morisseau C, Hammock BD. Impact of soluble epoxide hydrolase and epoxyeicosanoids on human health. Annual review of pharmacology and toxicology. 2013; 53:37–58.

Morisseau C, Inceoglu B, Schmelzer K, Tsai HJ, Jinks SL, Hegedus CM, Hammock BD. Naturally occurring monoepoxides of eicosapentaenoic acid and docosahexaenoic acid are bioactive antihyperalgesic lipids. J Lipid Res. 2010; 51:3481–3490. [PubMed: 20664072]

Morisseau C, Newman JW, Wheelock CE, Hill T, Morin D, Buckpitt AR, Hammock BD. Development of metabolically stable inhibitors of mammalian microsomal epoxide hydrolase. Chemical Research in Toxicology. 2008; 21:951–957. [PubMed: 18363382]

Mumby SM, Hammock BD. Partition assay for epoxide hydrases acting on insect juvenile hormone and an epoxide-containing juvenoid. Analytical Biochemistry. 1979; 92:16–21. [PubMed: 426275]

Nesvizhskii AI, Keller A, Kolker E, Aebersold R. A statistical model for identifying proteins by tandem mass spectrometry. Anal Chem. 2003; 75:4646–4658. [PubMed: 14632076]

Newman JW, Morisseau C, Hammock BD. Epoxide hydrolases: their roles and interactions with lipid metabolism. Progress in Lipid Research. 2005; 44:1–51. [PubMed: 15748653]

Node K, Huo Y, Ruan X, Yang B, Spiecker M, Ley K, Zeldin DC, Liao JK. Anti-inflammatory properties of cytochrome P450 epoxygenase-derived eicosanoids. Science. 1999; 285:1276–1279. [PubMed: 10455056]

Ollis DL, Cheah E, Cygler M, Dijkstra B, Frolow F, Franken SM, Harel M, Remington SJ, Silman I, Schrag J, Sussman JL, Verschueren KHG, Goldman A. The α/β hydrolase fold. Protein engineering. 1992; 5:197–211. [PubMed: 1409539]

Olsen KW, Moras D, Rossmann MG. Sequence variability and structure of D-glyceraldehyde-3-phosphate dehydrogenase. Journal of Biological Chemistry. 1975; 250:9313–9321. [PubMed: 1104621]

Pakpour N, Akman-Anderson L, Vodovotz Y, Luckhart S. The effects of ingested mammalian blood factors on vector arthropod immunity and physiology. Microbes and Infection. 2013; 15:243–254. [PubMed: 23370408]

Prestwich GD, Wojtasek H, Lentz AJ, Rabinovich JM. Biochemistry of proteins that bind and metabolize juvenile hormones. Archives of Insect Biochemistry and Physiology. 1996; 32:407–419. [PubMed: 8756303]

Richman AM, Dimopoulos G, Seeley D, Kafatos FC. *Plasmodium* activates the innate immune response of *Anopheles gambiae* mosquitoes. The EMBO journal. 1997; 16:6114–6119. [PubMed: 9321391]

Saitou N, Nei M. The neighbor-joining method - a new method for reconstructing phylogenetic trees. Molecular Biology and Evolution. 1987; 4:406–425. [PubMed: 3447015]

Schmelzer KR, Kubala L, Newman JW, Kim I-H, Eiserich JP, Hammock BD. Soluble epoxide hydrolase is a therapeutic target for acute inflammation. Proceedings of the National Academy of Sciences of the United States of America. 2005; 102:9772–9777. [PubMed: 15994227]

Seino A, Ogura T, Tsubota T, Shimomura M, Nakakura T, Tan A, Mita K, Shinoda T, Nakagawa Y, Shiotsuki T. Characterization of juvenile hormone epoxide hydrolase and related genes in the larval development of the silkworm *Bombyx mori*. Bioscience Biotechnology and Biochemistry. 2010; 74:1421–1429.

Severson TF, Goodrow MH, Morisseau C, Dowdy DL, Hammock BD. Urea and amide-based inhibitors of the juvenile hormone epoxide hydrolase of the tobacco hornworm (*Manduca sexta* : Sphingidae). Insect Biochemistry and Molecular Biology. 2002; 32:1741–1756. [PubMed: 12429126]

Silverman N, Maniatis T. NF-κB signaling pathways in mammalian and insect innate immunity. Genes & Development. 2001; 15:2321–2342. [PubMed: 11562344]

Stanley D. Prostaglandins and other eicosanoids in insects: Biological significance. Annual Review of Entomology. 2006:25–44.

Stanley D, Kim Y. Eicosanoid signaling in insects: from discovery to plant protection. Critical Reviews in Plant Sciences. 2014; 33:20–63.

Stanley DW, Miller JS. Eicosanoid actions in insect cellular immune functions. Entomologia Experimentalis Et Applicata. 2006; 119:1–13.

Surachetpong W, Singh N, Cheung KW, Luckhart S. MAPK ERK signaling regulates the TGF-beta 1-dependent mosquito response to *Plasmodium falciparum*. Plos Pathogens. 2009; 5(4)

Tamura K, Peterson D, Peterson N, Stecher G, Nei M, Kumar S. MEGA5: molecular evolutionary genetics analysis using maximum likelihood, evolutionary distance, and maximum parsimony methods. Molecular Biology and Evolution. 2011; 28:2731–2739. [PubMed: 21546353]

Taniai K, Inceoglu AB, Yukuhiro K, Hammock BD. Characterization and cDNA cloning of a clofibrate-inducible microsomal epoxide hydrolase in *Drosophila melanogaster*. European Journal of Biochemistry. 2003; 270:4696–4705. [PubMed: 14622257]

Tapiero H, Nguyen Ba G, Couvreur P, Tew KD. Polyunsaturated fatty acids (PUFA) and eicosanoids in human health and pathologies. Biomedicine & Pharmacotherapy. 2002; 56:215–222. [PubMed: 12199620]

Touhara K, Soroker V, Prestwich GD. Photoaffinity-labeling of juvenile hormone epoxide hydrolase and JH-binding proteins during ovarian and egg development in *Manduca sexta*. Insect Biochemistry and Molecular Biology. 1994; 24:633–640.

Tsubota T, Nakakura T, Shiotsuki T. Molecular characterization and enzymatic analysis of juvenile hormone epoxide hydrolase genes in the red flour beetle *Tribolium castaneum*. Insect Molecular Biology. 2010; 19:399–408. [PubMed: 20337748]

Vizioli J, Bulet P, Charlet M, Lowenberger C, Blass C, Muller HM, Dimopoulos G, Hoffmann J, Kafatos FC, Richman A. Cloning and analysis of a cecropin gene from the malaria vector mosquito, *Anopheles gambiae*. Insect Mol Biol. 2000; 9:75–84. [PubMed: 10672074]

Weyer U, Knight S, Possee RD. Analysis of very late gene expression by *Autographa californica* nuclear polyhedrosis virus and the further development of multiple expression vectors. The Journal of general virology. 1990; 71:1525–1534. [PubMed: 2197369]

WHO. World malaria Report 2012. World Health Organization; 2012.

Yu ZG, Xu FY, Huse LM, Morisseau C, Draper AJ, Newman JW, Parker C, Graham L, Engler MM, Hammock BD, Zeldin DC, Kroetz DL. Soluble epoxide hydrolase regulates hydrolysis of vasoactive epoxyeicosatrienoic acids. Circulation Research. 2000; 87:992–998. [PubMed: 11090543]

Zeldin DC, Kobayashi J, Falck JR, Winder BS, Hammock BD, Snapper JR, Capdevila JH. Regiofacial and enantiofacial selectivity of epoxyeicosatrienoic acid hydration by cytosolic epoxide hydrolase. Journal of Biological Chemistry. 1993; 268:6402–6407. [PubMed: 8454612]

Zhang QR, Xu WH, Chen FS, Li S. Molecular and biochemical characterization of juvenile hormone epoxide hydrolase from the silkworm, *Bombyx mori*. Insect Biochemistry and Molecular Biology. 2005; 35:153–164. [PubMed: 15681225]

Zhang WR, Koerner IP, Noppens R, Grafe M, Tsai HJ, Morisseau C, Luria A, Hammock BD, Falck JR, Alkayed NJ. Soluble epoxide hydrolase: a novel therapeutic target in stroke. Journal of Cerebral Blood Flow and Metabolism. 2007; 27:1931–1940. [PubMed: 17440491]

Highlights

- An epoxide hydrolase from the malaria mosquito *Anopheles gambiae* has been expressed in insect Sf-9 cells by the baculovirus expression system.
- The AgEH is a homolog of mammalian soluble epoxide hydrolases.
- The AgEH shows evolutionary, biochemical and immunological similarities to mammalian soluble epoxide hydrolases.
- The biochemical characterization suggested that epoxy fatty acids may be chemical mediators in mosquitoes that are metabolized by the AgEH.
- A nomenclature based on evolutionary history of epoxide hydrolases was updated.

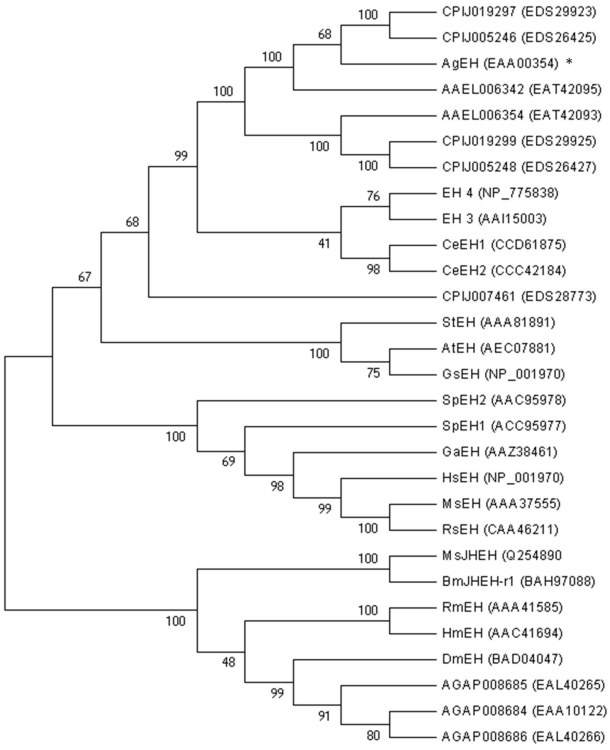

Fig. 1.

Phylogeny tree of the AgEH and other epoxide hydrolases from plants, insects, nematodes, sea urchins, chickens and mammals. The tree was generated by MEGA 5.2.1 (Tamura et al., 2011). The full names of abbreviations are detailed in the paper. The accession number of amino acid sequences is shown in the parenthesis. The percentage of replicate trees in which the associated taxa clustered together in the bootstrap test (1000 replicates) is shown next to the branches.

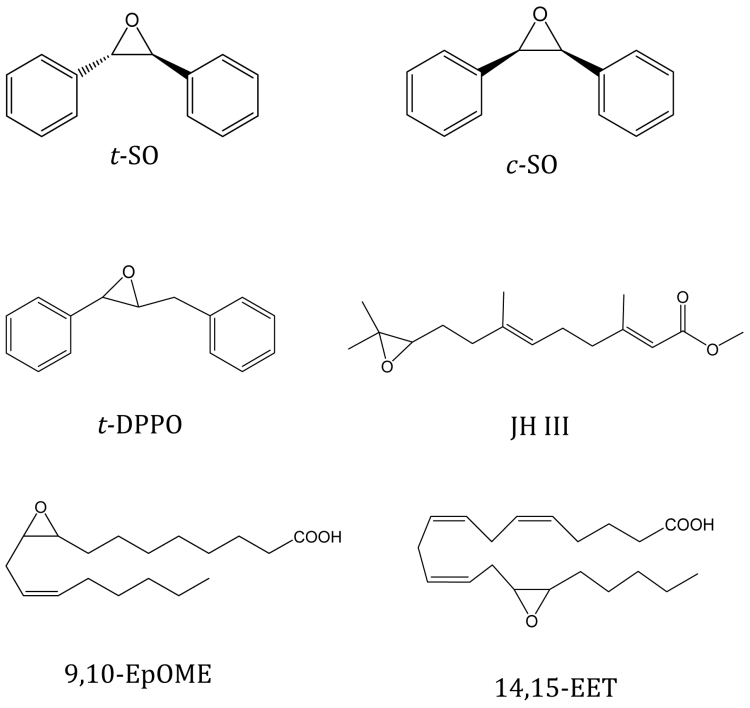

Fig. 2.

Epoxide containing substrates evaluated in the study. The full names of the substrates are detailed in the text.

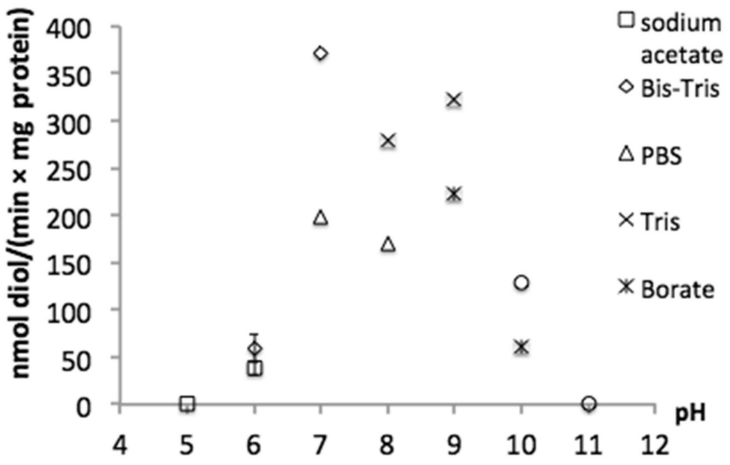

Fig. 3.

Effects of pH and buffer composition on enzyme activity. Enzyme activity was measured with *t*-DPPO as the substrate with triplicate assays. Data represent mean ± SD (n=3) except when SD is smaller than the datum point.

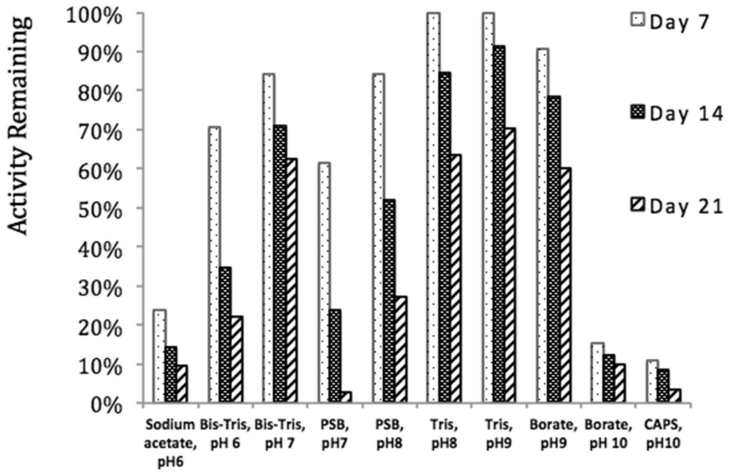

Fig. 4.

Enzyme stability in different buffers and pHs. The enzyme was stored in a bucket of crushed ice at a 4 °C freezer. Enzyme activity was measured with *t*-DPPO as the substrate with triplicate assays. Data represent the percentage of activity remaining (activity at day 1 is assigned 100%).

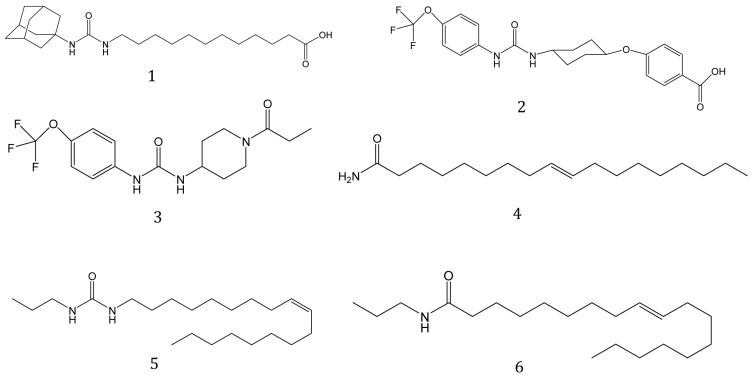

Fig. 5.

Inhibitors of the sEH (1-3) and mEH (4-6) used in the study. AUDA, *t*-TUCB and TPPU (#1 to #3) are urea-based mammalian sEH inhibitors (Morisseau et al., 1999). Elaidamide (#4) is a potent microsomal EH inhibitor (Morisseau et al., 2008). #5 and #6 are two potent inhibitors for the JHEH from *Manduca sexta* (Severson et al., 2002).

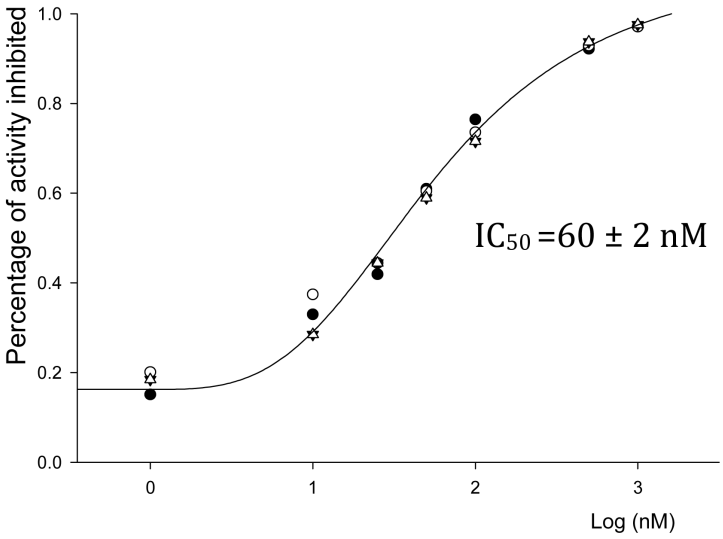

Fig. 6.

IC_{50} of AUDA (Compound 1 in Fig. 5) on the AgEH's activity on 14,15-EET. The 4 parameter logistic model describes the sigmoid-shaped response was used to calculate the IC_{50} (SigmaPlot, C.A)

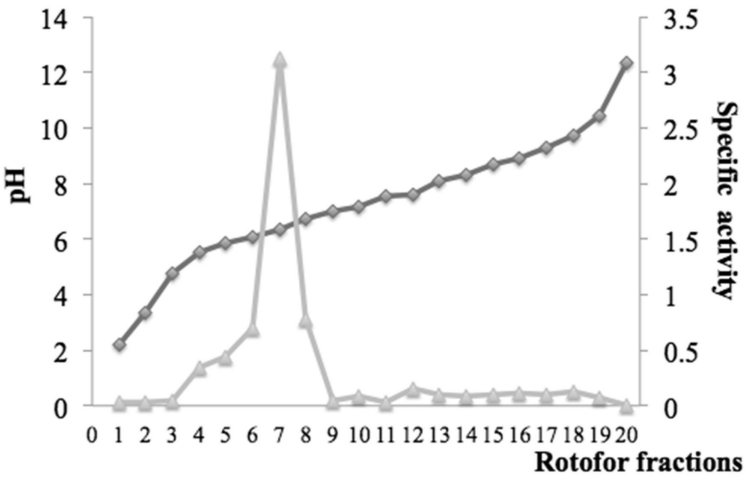

Fig. 7.

pH gradient and specific activity of Rotofor fractions. pH of fractions were measured, and 100 l of each fraction was diluted with 900 l 50 mM Tris-HCl, pH 8 buffer before activity was measured. Specific activity (mol diols/ (min × mg protein)) was measured with *t*-DPPO as the substrate. The pI determined was 6.3.

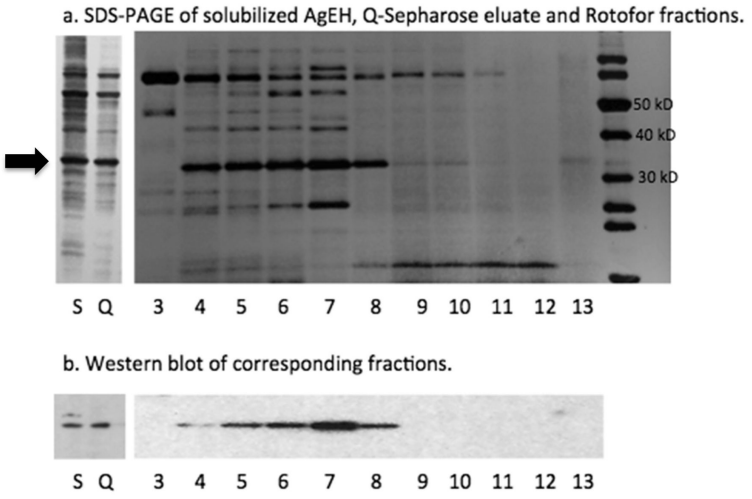

Fig. 8.

SDS-PAGE (a) and western blot analysis (b) of Rotorfor fractions.1 g of solubilized enzymes (S), Q-Sepharose eluate (Q) and Rotofor fractions #3 - #13 were loaded on a 4-20% Trisglycine gel (a). The proteins were also transferred to a nitrocellulose membrane and blotted against the rabbit serum against mouse sEH (b). The membrane was exposed to an X-ray film in a dark room for one minute.

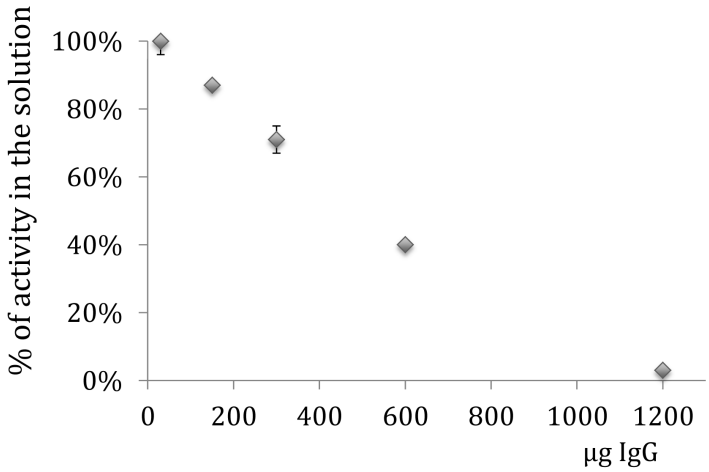

Fig. 9.

Immunoprecipitation of the AgEH activity. 100% activity refers to the amount of activity in the solution from non-immune IgG coupled agarose. Solubilized AgEH was subjected to immunoprecipitation with rabbit serum against mouse soluble epoxide hydrolase. Different amount of IgG were bound to Pierce protein A/G resin plus agarose. Enzyme solutions were added, and incubated with gentle end-over-end mixing overnight at 4 °C before activity in the solution was measured with *t*-DPPO as the substrate.

Table 1

Substrate selectivity of the AgEH.

Substrate	Specific Activity (nmol diol formed/(min × mg protein))
c-SO	<0.03
t-SO	<0.03
t-DPPO	564±80
JH III	98±2
14,15-EET	550±70
9,10-EpOME	360±50

Crude insect cell lysate was used for the assays. The enzyme assays were performed in 50 mM Tris-HCl, pH 8.0 containing 50 M substrates (5 M for JH III), 1% (v:v) DMSO and 0.1 mg/ml BSA at 30 °C. Data represent mean activity ± SD (n=3). No activity on *c*-SO and *t*-SO was detected, and the limit of detection is shown instead.

Table 2

The subcellular locations of the AgEH.

Cell fractions	Volume (ml)	Protein Concentration (mg/mL)	Activity (μmol/min)	Percent of total activity	Specific Activity (U/mg protein)
Crude lysate	20	0.91	4.2±0.2	100%	0.23±0.01
Mitochondria, Peroxisomes	10	0.36	1.15±0.04	27%	0.29±0.01
Cytosol	19	0.55	0.14±0.05	3%	0.01±0.004
Microsomes	10	0.28	2.0±0.3	48%	0.7±0.1

Enzyme activity from crude cell lysate is assigned as 100%. 1 U equals 1 mol/min. Insect sf-9 cells were infected by 10 M.O.I viruses, and harvested at 48 hours post infection. Enzyme activity was measured with *t*-DPPO as the substrate in triplicate assays. The values are the mean ± SD (n=3). Crude lysate refers to cell crude extract after cell disruption by a Polytron homogenizer. The other fractions are defined by centrifugal speed described in ‘Materials and methods’.

Table 3

Inhibition of the AgEH by sEH, mEH or JHEH inhibitors.

Inhibitors	*t*-DPPO			JH III			14,15-EET		
	5nM	50nM	500nM	5nM	50nM	500nM	5nM	50nM	500nM
1	44.9	9.5	N.D.	57.2	11.2	4.7	79.0	34.7	7.1
2	90.4	57.3	12.5	96.3	85.2	34.3	98.4	91.0	60.3
3	99.5	94.0	81.8	100	98.9	100	100	100	100
4	98.6	79.2	60.6	100	98.8	96.4	100	100	95.4
5	20.4	8.7	N.D.	70.3	45.9	22.6	100	86.3	32.3
6	50.6	28.7	8.6	94.7	70.2	50.7	100	100	64.0

Values are % of activity remaining with the presence of inhibitors. Inhibitors in DMSO were added, and incubated for 5 minutes before substrates were added into enzyme solutions. Enzymes from the microsomal fraction were used. Inhibition assays were done with triplicate assays. The SDs (n=3) are all within 10% of the mean value, and are not shown in the table. The enzyme assays were performed in 50 mM Tris-HCl, pH 8.0 containing 50 M substrates (5 M for JH III), inhibitors, 1% (v:v) DMSO and 0.1 mg/ml BSA at 30 °C.

Table 4

Enzyme kinetics of the AgEH on four epoxide hydrolase substrates.

Substrate	Kinetic parameter	AgEH	MsJHEH[a]	hsEH
	K_m (μM)	30.5±5.0	65.6	6.2±0.6[b]
t-DPPO	V_{max}(μmol × min^{-1}× mg^{-1})	1.2±0.1	0.059	2.1±0.1
	V_{max}/K_m(L × min^{-1}× mg^{-1})	0.041	0.0009	0.34
	K_m (μM)	7.0±0.6		2.6±0.4[b]
9,10-EpOME	V_{max}(μmol × min^{-1}× mg^{-1})	1.5±0.4	N.A.	0.35±0.03
	V_{max}/K_m(L × min^{-1}× mg^{-1})	0.21		0.13
	K_m (μM)	9.8±2.0	0.28	1.5±0.6
JH III	V_{max}(μmol × min^{-1}× mg^{-1})	1.3±0.1	0.095	0.067±0.007
	V_{max}/K_m (L × min^{-1}× mg^{-1})	0.13	0.34	0.04
	K_m (μm)	3.0±0.3		7.0±0.3[b]
14,15-EET	V_{max}(μmol × min^{-1}× mg^{-1})	1.4±0.03	N.A	1.4±0.05
	V_{max}/K_m(L × min^{-1}× mg^{-1})	0.46		0.20

Enzymes from the microsomal fractions were used for kinetics.

[a]The kinetics of MsJHEH on *t*-DPPO and JH III are from Severson and Touhara respectively (Severson et al., 2002; Touhara et al., 1994). N.A. indicates data are not available for the substrate.

[b]The kinetics of human sEH on *t*-DPPO, 9,10-EpOME and 14,15-EET are from Morisseau (Morisseau et al., 2000; Morisseau et al., 2010).

Table 5

Attempts to release the AgEH activity from the microsomal membrane by treatments of salts, urea and sonication.

Treatment	% of activity recovered from treatment	% of activity remaining in the microsomes
washed microsomes	100	86±5
+ 1M NaCl	94±2	92±4
+1M Urea	88±2	81±2
+3 X 30s Sonication	90±1	85±6

Microsomes were prepared and subjected by the corresponding treatments above. They were then repelleted and washed once with Tris buffer before *t*-DPPO activity was measured in the resulting pellets and supernatant. Values are means ± SD (n=3).

Table 6

Solubilization of the AgEH activity by CHAPS and Triton X-100.

CHAPS Percentage	Activity (μmol diol/min) in the pellet	Activity (μmol diol/min) in the supernatant	Recovery of activity after treatment (%)	% of activity in the supernatant
0.01%	0.08±0.003	0.002±0.0001	100	2
0.02%	0.07±0.001	0.006±0.0003	93	8
0.07%	0.06±0.007	0.009±0.0008	84	13
0.1%	0.06±0.002	0.01±0.0003	85	14
0.2%	0.04±0.001	0.015±0.002	67	27
0.3%	0.01±0.004	0.03±0.002	49	75
0.4%	0.007±0.001	0.015±0.004	27	68
0.5%	N.D.	N.D.	0	0
0.01%	0.08±0.003	0.003±0.0001	100	4
0.02%	0.06±0.002	0.015±0.0004	91	18
0.07%	0.05±0.004	0.018±0.0005	83	26
0.1%	0.04±0.001	0.02±0.003	72	33
0.2%	0.03±0.003	0.009±0.0001	48	23
0.3%	0.009±0.0008	0.001±0.0001	12	10

The activity in microsomes with 0.01% detergent was assigned 100% activity. The pellets were incubated with detergent at 4°C for one hour and re-pelleted. The critical micelle concentration (CMC) of CHAPS and Triton X-100 is 8-10 mM (0.4920-0.6150%, w/v) and 0.22-0.24 mM (0.013%-0.015%, w/v) respectively.

Table 7

Partial purification of the recombinant AgEH.

	Volume (mL)	Total protein (mg)	Total Activity (μmol/min)	Specific Activity (U/mg protein)	Yield (%)	Purification factor
Solubilized fraction	40	282	52	0.18	100	1
Q-Sepharose	20	114	35	0.31	67	1.7
Rotofor fraction #7	3	1.6	5	3.13	10	17

t-DPPO was used as the substrate. 1 U is 1 mol /min. 20 fractions were collected from Rotofor cell and fraction #7 is shown because it has the highest specific activity.